

Atomic resolution ultrahigh vacuum scanning tunneling microscopy of epitaxial diamond (100) films

R. E. Stallcup, A. F. Aviles, and J. M. Perez

Citation: *Appl. Phys. Lett.* **66**, 2331 (1995); doi: 10.1063/1.113973

View online: <http://dx.doi.org/10.1063/1.113973>

View Table of Contents: <http://apl.aip.org/resource/1/APPLAB/v66/i18>

Published by the [American Institute of Physics](http://www.aip.org).

Related Articles

Subwavelength nanopatterning of photochromic diarylethene films

Appl. Phys. Lett. **100**, 183103 (2012)

Metal-insulator transition with multiple micro-scaled avalanches in VO₂ thin film on TiO₂(001) substrates

Appl. Phys. Lett. **100**, 173112 (2012)

FeNi-based magnetoimpedance multilayers: Tailoring of the softness by magnetic spacers

Appl. Phys. Lett. **100**, 162410 (2012)

Optical dielectric behaviors of copper zinc alloy thin films

J. Appl. Phys. **111**, 073103 (2012)

Effect of Si interlayers on the magnetic and mechanical properties of Fe/Ge neutron polarizing multilayer mirrors

J. Appl. Phys. **111**, 063904 (2012)

Additional information on *Appl. Phys. Lett.*

Journal Homepage: <http://apl.aip.org/>

Journal Information: http://apl.aip.org/about/about_the_journal

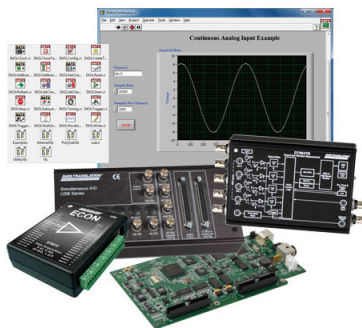
Top downloads: http://apl.aip.org/features/most_downloaded

Information for Authors: <http://apl.aip.org/authors>

ADVERTISEMENT

More Than 150
USB DAQ Modules

With Windows 7
and LabVIEW Support



DATA TRANSLATION®
www.datatranslation.com

Atomic resolution ultrahigh vacuum scanning tunneling microscopy of epitaxial diamond (100) films

R. E. Stallcup,^{a)} A. F. Aviles, and J. M. Perez

Physics Department, University of North Texas, Denton, Texas 76203

(Received 30 November 1994; accepted for publication 3 March 1995)

We report atomic resolution images of chemical vapor deposition grown epitaxial diamond (100) films obtained in ultrahigh vacuum (UHV) with a scanning tunneling microscope. A (2×1) dimer surface reconstruction and amorphous atomic regions are observed. The (2×1) unit cell is measured to be $0.51 \pm 0.01 \times 0.25 \pm 0.01$ nm². The amorphous regions are identified as amorphous carbon. A radial structure 1.5 nm in diameter is observed on a plane at a 20° slope to the (2×1) surface. Tunneling current versus voltage spectra in UHV and Raman spectra are also obtained. © 1995 American Institute of Physics.

Diamond films grown using chemical vapor deposition (CVD) have a great number of applications from cutting instruments to electronic components. Large single crystals of diamond would have applications in optical windows, electro-optical components, and integrated circuits. Currently, growth of large crystals using CVD has proven to be difficult.¹ Understanding the CVD diamond growth process at the atomic level is crucial in successfully producing large crystals in high volume. A basic assumption concerning the CVD diamond growth process is that it involves the formation of amorphous carbon and other carbon complexes on the growth surface.²⁻⁴ Recently, scanning tunneling microscopy (STM) in air has been used to observe parallel lines at equal distance along two orthogonal directions on a CVD grown diamond (100) surface known by using electron diffraction techniques to have a (2×1) reconstruction.⁵ STM in ultrahigh vacuum (UHV) has been ideal for studying the growth process at the atomic level of Si, Ge, and GaAs.⁶ STM in UHV has many advantages over STM in air such as surface cleanliness and the possibility of the use of etched tungsten tips that result in sharper images. Tunneling current versus voltage (*I*-*V*) spectroscopy using STM is also more reliable in UHV.⁶ In this letter, we report, for the first time, UHV STM studies of CVD grown epitaxial diamond (100) films. We directly observe a (2×1) surface reconstruction due to dimerization, and measure the (2×1) unit cell to be $0.51 \pm 0.01 \times 0.25 \pm 0.01$ nm². Moreover, we report the observation of amorphous atomic regions on the (2×1) reconstructed surface. The amorphous regions consist of linear structures surrounded by particles without any order. These regions resemble *sp*² and *sp*³ bonded carbon in amorphous carbon reported by Cho *et al.*⁷ using STM in air. *I*-*V* spectra obtained in UHV show that the surface of the film is *p*-type and has an electronic state 0.52 eV above the Fermi level.

The epitaxial film was grown on a polished 0.25×1.5×1.5 mm³ (100) type 2b high-pressure, high-temperature (HPHT) grown diamond substrate purchased from Harris Corporation. The substrate was cleaned ultrasonically in acetone, and then in a mixture of HCl and HNO₃ (1:3), and rinsed in triple distilled water. Using a hot-tungsten filament

CVD reactor, a conducting diamond film 1–2 μm thick was deposited on the substrate surface. The reactor is coupled to the UHV STM chamber via an all-metal through valve, and the samples are transferred from the reactor to the UHV STM chamber without contamination by exposure to air.⁸ The thin diamond film was deposited for 120 minutes with a substrate temperature of 850 °C at a pressure of 30 Torr using hydrogen and methane with flow rates of 200 and 1 sccm, respectively. The tungsten filament temperature was 2200 °C. The growth experiment was terminated by first shutting off only the methane flow and maintaining the sample, filament, and H₂ settings for 2 minutes. The filament was then turned off followed by the sample heater and then the H₂ flow being turned off. The images were obtained in UHV at a pressure of 1.0×10^{-10} Torr using an Aris 5000 UHV compatible STM from Burleigh Instruments. The STM probe was constructed of 20 mil tungsten wire and was electrochemically etched in a KOH solution.⁹ Tunneling currents of 2.8 nA with a sample bias of –800 mV were used to obtain atomic resolution. *I*-*V* spectroscopy in UHV was obtained using the same image scan parameters (current and sample bias) stated previously.

Figure 1(a) shows a UHV STM image of the diamond (100) epitaxial film having a (2×1) dimer reconstruction of the surface. Steps are observed consisting of atomic planes with dimer rows rotated in the *xy*-plane 90° relative to the dimer rows in the upper or lower atomic planes. Images of the diamond surface on an atomic scale in UHV were easily reproducible. A dimer-type reconstruction has been hypothesized for the diamond (100) (2×1) surface, but the dimers have not been directly observed previously.⁵ In the present experiments, the spacings between dimers within a row were measured at higher resolution, as shown in Fig. 1(b), thus directly confirming the dimerization of the (2×1) surface. From Fig. 1(b), the (2×1) unit cell is measured to be $0.51 \pm 0.01 \times 0.25 \pm 0.01$ nm², in agreement with the diamond (100) (1×1) lattice constant of 0.252 nm. The step heights in Fig. 1(a) are measured to be 0.10 ± 0.01 nm, in agreement with the reported spacing between diamond (100) planes of 0.089 nm. In Fig. 1(a), particles grouped together in clusters with little or no apparent order are observed at the edges of the steps on the right-hand side of the figure. Other regions of the film showed ordered linear chains of particles with

^{a)} Electronic mail: stallcup@ponder.csci.unt.edu

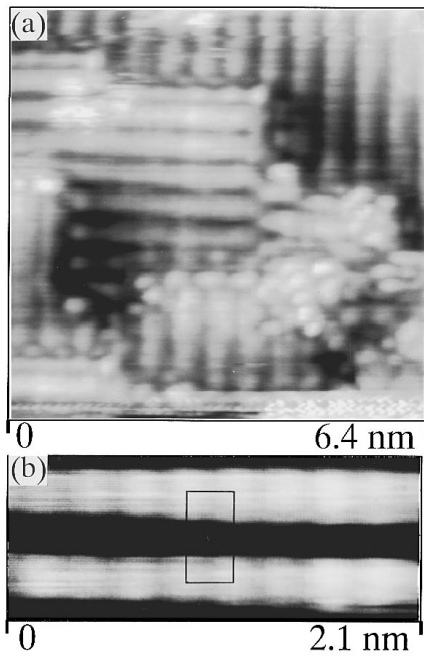


FIG. 1. (a) UHV STM atomic resolution image of a CVD grown epitaxial diamond (100) film. A (2×1) dimer surface reconstruction is observed. Clusters of particles with little or no apparent order are also observed on the right-hand side. (b) UHV STM image of dimer rows showing the individual dimers within the rows.

disordered groups of particles, as shown in Fig. 2(a). These structures are similar to those reported in amorphous carbon by Cho *et al.*⁷ using STM in air. The lattice spacings of the linear chains in Fig. 2(a) are measured to be 0.35 ± 0.01 nm and 0.26 ± 0.01 nm along the long and short axis, respectively. These measurements are in excellent agreement with the spacings of 0.35 ± 0.01 nm and 0.28 ± 0.01 nm reported for the linear chains in amorphous carbon.⁷ We therefore attribute the amorphous regions to amorphous carbon. In Ref. 7, the ordered linear chains are attributed to a form of sp^2 bonded graphite and the disordered regions to a random network of sp^3 bonded carbon. Random networks of sp^2 and sp^3 bonded carbon atoms have been predicted to form in polycrystalline diamond films based on Raman spectroscopy.¹⁰ Approximately 20% of the diamond film surface was observed to consist of the amorphous regions described above.

Radial structures are also observed on the (100) surface at steps, as indicated by the arrow in Fig. 2(b). One would not expect to observe a reconstruction of the diamond (100) surface to have this geometric shape. After further analysis, it is found that the steps in Fig. 2(b) are approximately 6 atomic layers high (0.06 nm) and the radial structure is at a 20° angle to the (100) plane. This structure could therefore be a reconstruction of a plane 20° to the (100) plane.

Large area STM images of $0.5\times 0.5 \mu^2$ show the surface of the film to be flat and epitaxial. We observe (100) planes with the same orientation stacked on one another and parallel to the substrate surface. The root-mean-squared roughness of a $3.4\times 3.4 \mu^2$ area is measured to be 90 nm.

Figure 3(a) shows the Raman spectrum of the diamond substrate before film growth obtained using a laser line of

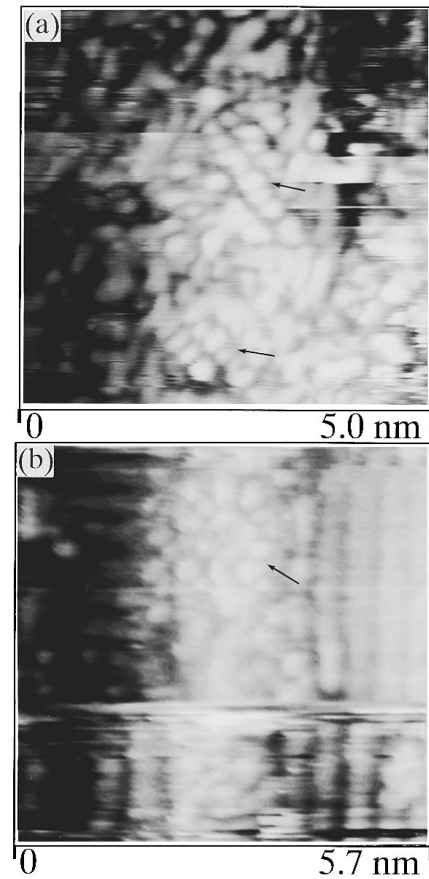


FIG. 2. (a) UHV STM atomic resolution image of a region of the same film showing an amorphous region consisting of ordered linear chains, indicated by the arrows, surrounded by particles without any order. (b) STM image of a radial structure, indicated by the arrow, on a plane at an angle of 20° to the (100) plane.

514.5 nm. The sp^2 carbon signal from the bulk at 1579 cm^{-1} is slightly above the baseline of the spectrum showing that there is very little graphitic carbon. Figure 3(b) shows the Raman spectrum of the epitaxial film after growth on this substrate. The sp^2 carbon signal at 1579 cm^{-1} has the same

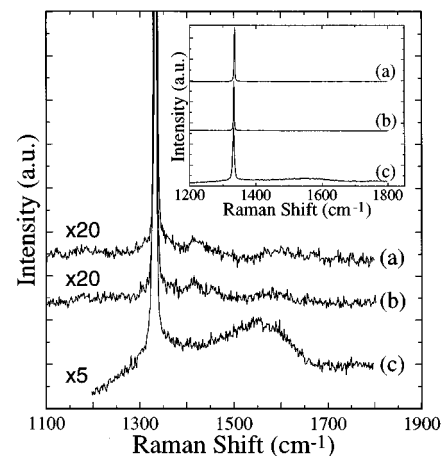


FIG. 3. (a) Raman spectrum of the diamond substrate before film growth. (b) Raman spectrum of the epitaxial film. (c) Raman spectrum of a polycrystalline film grown on Si. Inset shows the corresponding unexpanded Raman spectra.

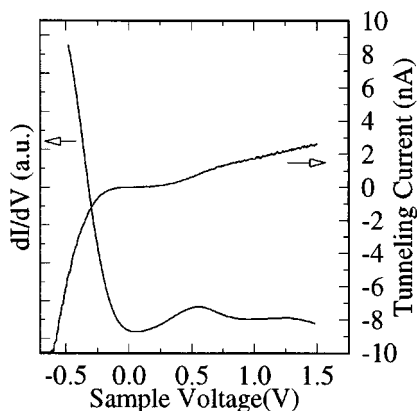


FIG. 4. Right-hand axis corresponds to the tunneling current vs sample voltage curve obtained in UHV with the STM tip over a dimer. The left-hand axis corresponds to the conductance, dI/dV , vs sample voltage curve showing a surface state +0.52 V above the Fermi level.

height and baseline before and after film growth, showing that the epitaxial diamond film does not contain any measurable graphitic carbon. In comparison, Fig. 3(c) shows the Raman spectrum of a polycrystalline diamond film grown on Si. Both films were grown using the same parameters to approximately the same thickness. In Fig. 3, the vertical axis is expanded to bring out the detail of the spectrum. The graphitic carbon in polycrystalline films on Si has been reported to form at grain boundaries¹¹ and the Si interface.¹² Since the Raman spectrum of the epitaxial film did not show any graphitic carbon, the amorphous carbon regions we observed on the film's surface using STM must be etched or converted to diamond and do not contribute to the bulk of the film during the growth process. This observation supports recent models for CVD diamond growth that involve the deposition of a graphitic carbon layer on the surface that is converted to diamond.⁴

Before film deposition it was not possible to obtain a tunneling current from the STM tip to the clean diamond substrate surface. This is due to the insulating nature of HPHT grown diamond. Tunneling is easily achieved after the CVD epitaxial diamond film is grown. The conduction mechanism is unknown. The high conductivity of CVD grown epitaxial diamond films has been previously reported and attributed to H incorporation in the lattice¹² or H termination of the surface.¹³ It has recently been reported that the formation of amorphous carbon on the surface of diamond by hydrogenation increases the conductivity.¹⁴ Thus the amorphous carbon regions we observed on the surface of the epitaxial film could be responsible for the conductivity. To investigate the electronic structure of the surface of the film, we obtained $I-V$ spectra in UHV with the STM tip over a dimer. Figure 4 shows a typical $I-V$ curve and conductance, dI/dV , versus voltage curve. The conductance for negative and positive sample voltages is proportional to the local sur-

face density of states below and above the Fermi level, respectively.⁶ The large conductance observed for negative sample voltages shows that the surface of the epitaxial film is p type, consistent with previous measurements using Hall effect and other techniques.¹⁵ A new peak is observed in the conductance at +0.52 V, showing a surface state 0.52 eV above the Fermi level.

In summary, we have reported the first atomic resolution UHV STM images of a CVD grown epitaxial diamond (100) film. We showed direct evidence for dimerization of the diamond (100) surface, thus confirming the hypothesis that the (2×1) reconstruction is due to dimerization. We observed amorphous regions on the (2×1) dimer reconstructed surface that we identified as amorphous carbon. This observation is direct evidence for the formation of amorphous carbon regions on the diamond growth surface during epitaxial growth. We are currently studying the evolution of these amorphous regions during the growth process using UHV STM. Understanding the growth process at the atomic scale will be the key in producing high quality diamond films for a wide range of applications.

This work was supported in part by the National Aeronautics and Space Administration under Award No. NAG-1-1468, the Texas Advanced Research Program under Award No. 003594053, and the National Science Foundation under Award No. DMR-9311724.

- ¹R. W. Pryor, M. W. Geis, and H. R. Clark, *Mater. Res. Soc. Symp. Proc.* **242**, 13 (1992).
- ²B. V. Deryagin and D. V. Fedoseev, in *Diamond Growth and Films* (Elsevier, New York, 1989), pp. 131–248.
- ³K. E. Spear and M. Frenklach, in *Synthetic Diamond: Emerging CVD Science and Technology*, edited by K. E. Spear and J. P. Dismukes (Wiley, New York, 1993), pp. 243–304.
- ⁴D. S. Olson, M. A. Kelly, S. Kapoor, and S. B. Hagstrom, *J. Mater. Res.* **9**, 1546 (1994).
- ⁵T. Tsuno, T. Imai, Y. Nishibayashi, K. Hamada, and N. Fujimori, *Jpn. J. Appl. Phys.* **30**, 1063 (1991).
- ⁶*Scanning Tunneling Microscopy*, edited by J. A. Stroscio and W. J. Kaiser (Academic, Boston, 1993).
- ⁷N. H. Cho, D. K. Veirs, J. W. Ager III, M. D. Rubin, and C. B. Hopper, *J. Appl. Phys.* **71**, 2243 (1992).
- ⁸J. M. Perez, W. Rivera, C. Lin, R. C. Hyer, M. Green, S. C. Sharma, D. R. Chopra, and A. R. Chourasia, in *Atomic Force/Scanning Tunneling Microscopy*, edited by S. Cohen, M. Bray, and M. Lightbody (Plenum, New York, 1994), pp. 203–210.
- ⁹P. J. Bryant, H. S. Kim, Y. C. Zheng, and R. Yang, *Rev. Sci. Instrum.* **58**, 1115 (1987).
- ¹⁰C. Wild, N. Herres, J. Wagner, P. Koidl, and T. Anthony, *Electrochem. Soc. Proc.* **89**, 283 (1989).
- ¹¹P. J. Fallon and L. M. Brown, *Diam. Relat. Mater.* **2**, 1004 (1994).
- ¹²D. A. Muller, Y. Tzou, R. Raj, and J. Silcox, *Nature (London)* **366**, 725 (1993).
- ¹³H. Shiomi, Y. Nishibayashi, and N. Fujimori, *Jpn. J. Appl. Phys.* **30**, 1363 (1991).
- ¹⁴T. Maki, S. Shikama, M. Komori, Y. Sakaguchi, K. Sakuta, and T. Kobayashi, *Jpn. J. Appl. Phys.* **31**, 1446 (1992).
- ¹⁵Y. Muto, T. Sugino, J. Shirafuji, and K. Kobashi, *Appl. Phys. Lett.* **59**, 843 (1991).